ELSEVIER

Journal of Nuclear Materials 290–293 (2001) 537–541

journal of nuclear materials

www.elsevier.nl/locate/jnucmat

Plasma edge fluid models for recycling at near tangential surfaces

M. Baelmans [a,*], D. Reiter [b,c], B. Küppers [c], P. Börner [c]

[a] *Department of Mechanical Engineering, Katholieke Universiteit Leuven, Celestijnenlaan 300A, B-3001 Leuven, Belgium*
[b] *Institut für Laser- und Plasmaphysik, Heinrich Heine Universität Düsseldorf, D-40225 Düsseldorf, Germany*
[c] *Association EURATOM-KFA, Institut für Plasmaphysik, Forschungszentrum Jülich GmbH, D-52425Jülich, Germany*

Abstract

2D-plasma edge fluid modeling has become a common tool to investigate aspects of plasma surface interaction (PSI) in fusion devices. Recycling at exposed surfaces is included, typically, via Bohm-type boundary conditions for the plasma flow field along the B-field. Only very crude prescriptions are in use for near tangential surfaces. Such structures are, however, crucial for limiter configurations, for the baffles in divertors and for main chamber recycling. Experimentally the recycling at such surfaces is often found to be much stronger than predicted if sheath theory is extrapolated to very small field line inclination angles. In this paper we present extensions of the B2-EIRENE code system to study such effects in detail, and we apply this to evaluate, quantitatively, some of the assumptions behind one particular ('funneling-') model proposed earlier for plasma fluxes onto tangential surfaces.

Keywords: Limiter; 2D model

1. Introduction

2D-plasma edge fluid codes such as the B2-EIRENE code versions, e.g., [1], typically use a Bohm-type sheath criterion as boundary conditions for the plasma flow along the B-field onto orthogonal or inclined surface targets [5,6]. However, both because of physical uncertainties and numerical restrictions the plasma flow onto near tangential solid structures is treated only quite poorly. This implies a severe conceptual limitation in the predictive quality of the model with regard to those physical effects, which originate from recycling at tangential limiter faces [8], at divertor baffling structures, at very strongly inclined divertor targets, or from main chamber recycling.

In order to improve this situation we have implemented into B2-EIRENE a modified numerical treatment of inclined (with respect to $\vec{B}$) target surfaces. Distinct from the conventionally used distortion of the orthogonal computational grid, [2] corrected by some 'ad hoc' modifications in the code, we retain the full orthogonallity of the grid except for the last cell in front of the target. In this last cell an adaptation of the finite volume discretization implemented in B2 permits a physically correct solution for plasma flow onto inclined targets without limitation in the field line inclination angle. The interfacing routine between B2 and EIRENE (segment INFCOP in EIRENE) [4] is generalized accordingly. We summarize these technical points in Appendix A. With these code extensions we are able to study effects of PSI at near tangential targets. In particular we assess some of the postulations behind a simple analytical 'funneling model' (FM) [7] and its consequences, by a full 2D plasma fluid simulation. This model was setup, originally, to explain discrepancies between experimentally observed plasma fluxes onto near tangential surfaces (e.g., the inner limiter at TFTR, or from tilted probe experiments, loc. cit.) and conventional geometrical arguments based upon a 1D parallel flow argument.

* Corresponding author. Tel.: +32-16 32 2517; fax: +32-16 32 2985.
E-mail address: martine.baelmans@mech.kuleuven.ac.be (M. Baelmans).

0022-3115/01/$ - see front matter
PII: S0022-3115(00)00517-1

In the next section we briefly summarize this particular 2D funneling model. In Section 3 we discuss its (partial) validation by showing that some of the postulations required for the analytical treatment and the basic conclusions can be recovered in a more complete 2D fluid simulation, in particular with a self-consistent ambipolar field, parallel forces, cross-field viscosity, etc. For this study we apply the extended B2 code to idealized 'blunt-nosed limiter' configurations.

Finally, we apply this to a more realistic limiter shape, namely to that of the ALT-II toroidal pump limiter in TEXTOR-94. In particular we assess the FM with respect to the reported discrepancy [8] between experimental and theoretical H-alpha emission profiles in front of the tangential limiter roof.

2. Stangeby's 'funneling model'

For all details of the discussion in this chapter we refer to Ref. [7]. The basic arguments are as follows: commonly adopted arguments of 1D parallel plasma flow results in a $\sin(\theta)$ dependence of the plasma deposition at surfaces, where θ is the angle between the $\vec{B}$-field and the surface normal. Let $2L_F$ be the length of the target front face aligned with the $\vec{B}$-field and L the connection length (i.e., $2L$ is the distance between limiters). Assuming poloidally constant cross-field transport $D_\perp$, a simple geometrical consideration of cross-field fluxes alone shows that a fraction $L_F/(L+L_F)$ of the total flux (Φ) through the separatrix will go directly onto the front face ($\Phi_\perp$), whereas the remaining fraction $L/(L+L_F)$ will be driven, by parallel forces, onto the limiter sides ($\Phi_\parallel$). Hence the ratio will be $\Phi_\perp/\Phi_\parallel = L_F/L$. Re-ionization of recycled particles is assumed to occur predominantly outside the region considered here, i.e., radially further inward. Both predictions are often in conflict with probe data and thermography or spectrography in front of limiters, loc.cit. and, e.g., Ref. [3] for a more recent experimental identification of that problem.

Combining the parallel and perpendicular considerations into a 2D picture as shown in Fig. 1, shows that this latter ratio is increased to $\Phi_\perp/\Phi_\parallel = \sqrt{L_F/L}$. The key assumption here is that: (a1) the sink action of the tangential limiter plane leads to a density depression in front of the target, (a2) the penetration length λ_f of the perturbation for density and parallel particle flux radially inward (inside the LCFS (last closed flux surface) are the same, (a3) re-ionisation of recycled neutrals occurs outside this region.

Furthermore, it is postulated: (b1) that this density depression is strong enough to induce sonic flow along $\vec{B}$ just inside the last closed flux surface near the limiter corners, with the sonic flow speed near the limiter corners extending inward also the same radial length λ_f, (b2) this induced parallel flow inside the LCFS is isothermal, (b3) parallel and cross-field viscosity are neglected.

In the following sections we will describe 2D plasma flow simulations in front of limiters, retaining postulates (a), but checking postulates (b), and the predictions of the FM, which result from the self-consistent 2D ambipolar field and fluid forces. We do this by enforcing a direct radial plasma flow onto aligned target surfaces, via boundary conditions locally imposing a certain convection velocity. Lacking a sheath theory or the equivalent of a Bohm-condition here, the value of this locally imposed radial velocity remains a free model parameter and is varied. The 2D plasma flow simulations show, however, that a saturation of fluxes $\Phi_\perp$ occurs with increasing imposed $v_\perp$ at the target (see below). Hence there is a maximum level of 'induced' plasma fluxes onto nearly tangential surfaces, corresponding to the idealized 2D funneling effect suggested in Ref. [7]. This can readily be implemented in plasma edge models via an iteration of the boundary condition of an imposed $v_\perp$ at (near) tangential targets.

Complementary to this 2D picture it has been speculated that, locally, enhanced cross-field diffusion or convection is caused by the presence of a solid surface in contact with the plasma. This can be assessed in edge codes by enhancing, locally, the $D_\perp$ in the plasma region in front of the limiter face. It would add to the 2D funnel effect studied here, but is not considered in this present work.

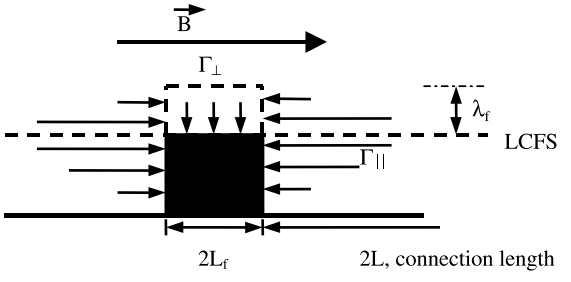

Fig. 1. Schematic view of the limiter configuration as described by the funneling model.

3. Application to an idealized 'blunt-nosed limiter'

In order to investigate the funneling effect within the frame of conventionally applied 2D plasma edge codes a simple toroidal limiter of rectangular shape in the poloidal (r,ϕ) plane is discussed here. In other words, only orthogonal and parallel surfaces with respect to the magnetic configuration are involved. The further model parameters have been selected to be typical for a medium-sized limiter tokamak, e.g., TEXTOR, but

these choices are irrelevant for the particular issue considered here.

The computational domain is an annular segment of nested concentric circular magnetic surfaces, representing the boundary plasma region of a tokamak. The inner radius (boundary to core plasma) is at 40 cm, the outer radius (the vacuum wall) is at 55 cm. The major radius of the torus is 1.75 m. The magnetic field was computed assuming a value of 2.25 T at the magnetic axis and a plasma current of 350 kA. The blunt-nosed limiter is positioned at the outer midplane, its aligned plasma facing surface is at $a = 45$ cm. The poloidal extent of that limiter was 33.75°. In addition a limiter with twice and halve that poloidal width is investigated.

The transport model chosen was a typical B2-EIRENE setup of 2D plasma edge flow simulations: For the parallel transport coefficients the Braginskii expressions are used with flux limiting factors for heat fluxes and parallel momentum of 0.2 and 0.4, respectively. The radial anomalous diffusion coefficient as well as the radial transport coefficients for parallel momentum, electron and ion energy are set equal 1 m^2/s, no cross-field convection was specified in the radial particle balance inside the computational domain.

On the magnetic flux surface at the **core plasma interface** following boundary conditions are used: $V_\theta = 0$ m/s; $n = 1.45 \times 10^{19}$ m^{-3}; $T_e = T_i = 110$ eV. At the **orthogonal targets**, plasma sheath edge conditions are imposed: $V_\theta = (B_\theta/B)c_s$; $Q^e_\theta = 4.8T_e nV_\theta$; $Q^i_\theta = 2.5T_i nV_\theta + \frac{1}{2}mnV^2_\parallel$. At the **tangential limiter face**, new boundary conditions are explored: V_r is imposed, and increased until saturation of $\Phi_\perp$ onto the aligned surface. $Q^e_r = 2T_e nV_r$ and $Q^i_\theta = 2T_i nV_r$. Lacking a generally accepted sheath theory for aligned surfaces, this guess is as good as any. For the boundary conditions at the **vacuum wall** again conventional specifications are used: $n = 2 \times 10^{17}$ m^{-3}; zero momentum transport to the wall; $T_e = 6$ eV and $T_i = 22$ eV.

Recycling of neutral particles was found to be irrelevant for the effects discussed here, as long as the majority of re-ionization occurred at a radial distance larger than λ_F. This latter recycling pattern resulted from the EIRENE Monte Carlo code for the conditions specified here, and for a wide range of recycling parameters in simple neutral models as well. Therefore, recycling will not be considered further here.

The particle flux towards the limiter head peaks near the limiter corners as shown in Fig. 2. Thus, computational results are likely to be quite vulnerable to numerical discretization errors. In order to eliminate such finite grid size effects, subsequently refined meshes are used in combination with the Richardson extrapolation technique [9].

Increasing the imposed radial convection velocity at the limiter roof (boundary condition) gives rise to a saturation in particle flux $\Phi_\perp$, see Fig. 3. At the same time, the ion density along the limiter head just inside the LCFS is found to be depressed by more than an order of magnitude, compared to the unperturbed value further upstream along the same flux tube (see Fig. 4). Near the limiter corners, sonic speed is reached, again inside the LCFS. This computational result is a direct confirmation of the postulates (b) of Ref. [7] mentioned above.

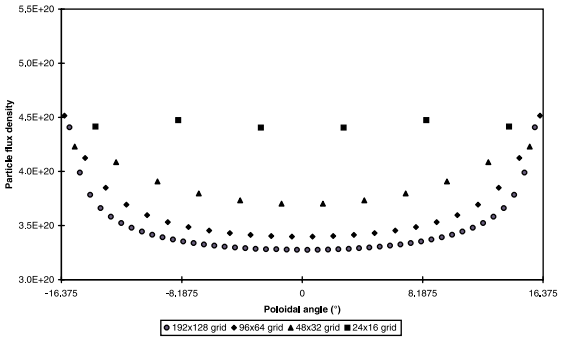

Fig. 2. Poloidal particle flux distributions to limiter head, grid sensitivity study. The number of grid cells is stepwise doubled ($24 \times 16, 48 \times 32, 96 \times 64, 192 \times 128$).

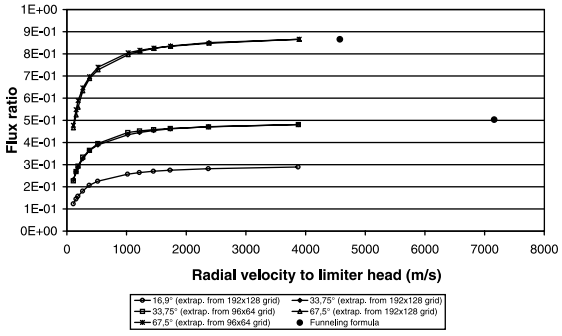

Fig. 3. Radial particle flux onto limiter showing saturation near analytic FM predictions for the highest imposed radial convection velocities. The three curves correspond to Richardson extrapolated curves for different limiter dimensions (16.9° for the lowest curve, 33.75° for the middle curve, 67.5° for the highest ratios). Also included with bullets are estimations for the funneling formula [5].

In addition to the 2D flow simulation, combined with extensive grid sensitivity studies to resolve peculiarities of the flow near the corners indicate that small values for the radial velocity (well below the speed required to achieve saturation of perpendicular fluxes) result in discontinuities in the parallel ion density profile near the corners as also shown in Fig. 4. Hence, we conclude that the runs with the full funneling effect (i.e., large imposed radial losses onto the target) are physically more relevant than those with the much lower values which would be inferred, e.g., from the simple 1D geometrical arguments given in Section 3.

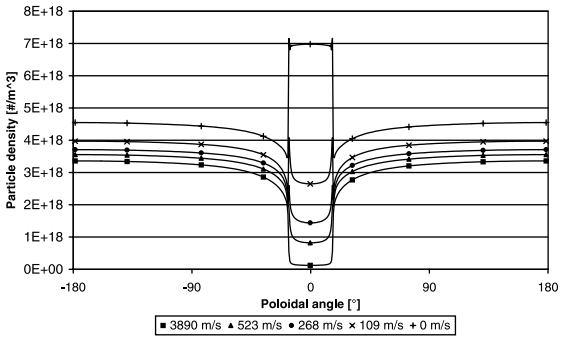

Fig. 4. Density profile along the separatrix for increasing imposed radial convection onto limiter face, showing strong density depression in front of the limiter.

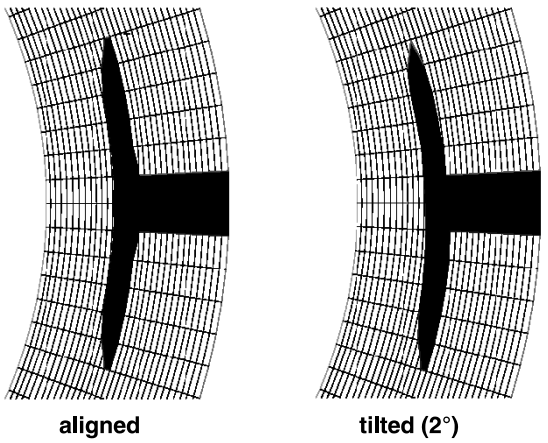

Fig. 5. Discretized geometry for ALT-II like simulations.

The plasma temperature profiles along the field, just inside the LCFS where the funneling flow is formed, are found to be fairly constant (hence confirming the isothermal flow assumption in [7], except for the region very close to the limiter corners, in which an adiabatic cooling (due to acceleration of the parallel flow) results. Furthermore, 2D code results lead to values for $\Phi_{\perp}/\Phi_{\parallel}$ of 0.29, 0.48, 0.87 for the halved, reference and double limiter, respectively. This is much closer to the FM predictions (0.22, 0.32, 0.48) than to the simple geometry argument (0.05, 0.10, 0.23) and, as expected, the effect is even stronger than the FM predictions, in particular for larger tangential surfaces. Finally, even the analytically predicted radial extend of the perturbation inside the LCFS is confirmed by the code results, both values are approximately 0.5 cm.

4. Application to an ALT-II like toroidal pump limiter configuration

The same B2-EIRENE setup was also applied to a more realistic limiter configuration. The limiter shape and radial position were chosen to match the ALT-II pump limiter of TEXTOR-94. As we wish to isolate the effects of the FM from geometric effects the limiter is moved into the midplane in our simulations, whereas the true position in TEXTOR is 45 degrees under the outer midplane.

The same modeling strategy has also been applied here, i.e. increasing the imposed cross-field convection onto the aligned or slightly misaligned limiter roof (see Fig. 5). Inclined targets are thereby handled by a combined parallel and radial flux as described in Appendix A.

Self-consistent recycling and funneling action is compared for a perfectly aligned and a slightly (2°) tilted ALT-II shaped limiter (see Fig. 6). We find, even in case of perfect alignment of the roof, a strong infilling of the gap in the poloidal recycling pattern which, however,

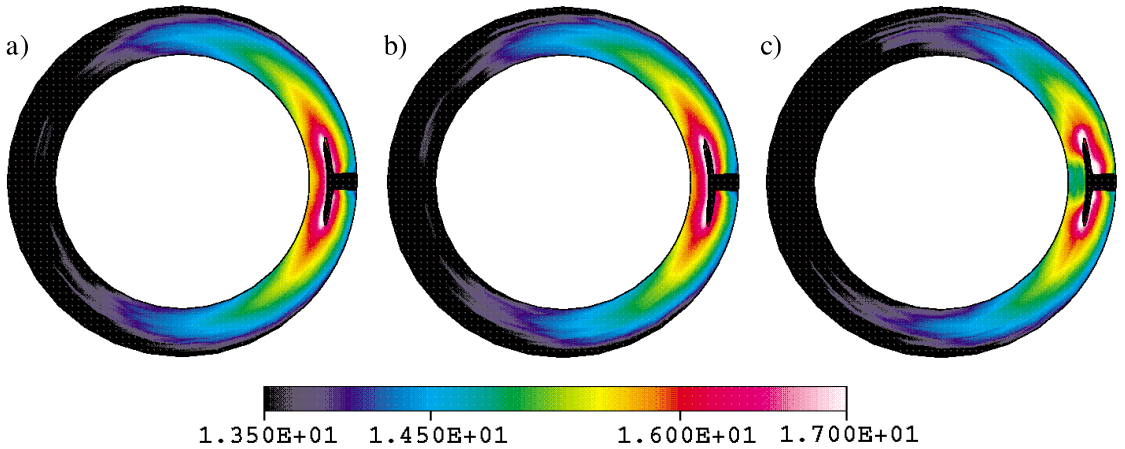

Fig. 6. Ion particle sources for different simulations: (a) aligned, (b) misaligned and (c) aligned, old B2-EIRENE model.

remains hollow between the limiter tips. Misalignment significantly adds to that infilling.

The experimental results reported in [8] (i.e. peak recycling (H_α) between the limiter tips) can, however, only be matched by either assuming misalignment of the limiter or strongly enhanced radial transport locally in front of the roof. This could easily have happened because the shape of ALT-II at the time of the measurements would have been aligned only at one particular radial position. The funneling alone, plus perfect alignment however is not quite sufficient, but in any case, very substantial for limiter recycling in general.

5. Conclusions

The B2-EIRENE code system has been extended to permit computational studies of PSI at strongly inclined, and even aligned target surfaces. A particular model for the nature of radial plasma fluxes is achieved. Hereby features of the analytical model as reported in [7] are, essentially, recovered. In particular B2-EIRENE results of limiter recycling and of divertor baffling will be significantly affected.

Appendix A. B2-EIRENE code extensions

The code is extended to take account for boundary conditions at convex material surfaces. Thus finite volume discretization results in corner cells which should be capable to handle two (different) boundary conditions. This is shown in Fig. 7. In the B2 procedure, additional boundary cells are provided with sources and sinks to obtain the required boundaries. In order to enforce the correct composition of the two flux components, the second boundary condition for the radial surfaces of corner cells is explicitly implemented.

At inclined boundaries parallel and radial flux contributions are accounted for. Total particle, electron and ion energy fluxes normal to the surface are computed as

$$\vec{\Gamma} \cdot \vec{S} = \Gamma_\theta S_\theta + \Gamma_r S_r. \tag{A.1}$$

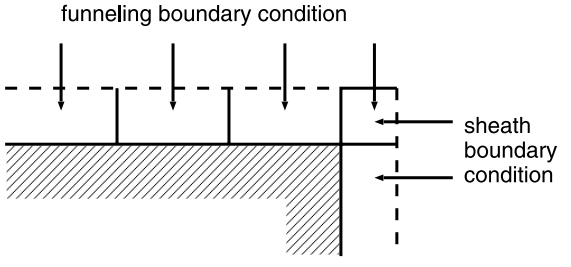

Fig. 7. Implementation of boundary conditions at convex material surfaces.

Local transport coefficients near inclined targets are adapted in order to reflect both parallel and radial transport near the inclined target. Indeed, normal transport towards an inclined boundary is governed by

$$\kappa_n \frac{\partial T}{\partial n}\overrightarrow{e_n} = \kappa_\theta \frac{\partial T}{\partial \theta}\overrightarrow{e_\theta} + \kappa_r \frac{\partial T}{\partial r}\overrightarrow{e_r} \tag{A.2}$$

leading to effective coefficients

$$\kappa_{\theta,\mathrm{eff}} = \kappa_\theta + \kappa_r \tan^2\alpha \quad \text{and} \quad \kappa_{r,\mathrm{eff}} = \frac{\kappa_\theta}{\tan^2\alpha} + \kappa_r. \tag{A.3}$$

The computational grid of B2 is also used to discretize the volume for the EIRENE Monte Carlo neutral particle simulation, which is carried out in Cartesian coordinates (x, y) in the poloidal plane, plus either a z-coordinate (cylindrical approximation) or a toroidal angle ϕ. EIRENE volume quantities (sources and sinks in the plasma flow equations) are integrals over the grid cells. Previously, the transformation of the B2 flow field and the $\vec{B}$ field into Cartesian coordinates was automatically performed from the grid data, assuming a perfectly aligned and orthogonal grid. This is now replaced by a more general option, in which the Cartesian components of the $\vec{B}$-field are provided to EIRENE from B2, in addition to the standard set of plasma- and grid data. Furthermore, at each cell face, now two (rather than only one, as previously) ion particle flux components are exchanged. From these the new B2-fluid boundary conditions at inclined targets described above are translated to drifting Maxwellians for each ion species. The simulation of the sheath has remained, as before, in the EIRENE code, i.e., the sheath potential drop calculated from the various ion flow velocities at the sheath entrance. The sheath is automatically set to zero for field line inclination angles below a critical value ($\theta_{\mathrm{crit}} = 0.5°$).

References

[1] D. Reiter, J. Nucl. Mater. 196–198 (1992) 241.
[2] R. Schneider, D. Reiter et al., J. Nucl. Mater. 196–198 (1992).
[3] D. Guilham et al., J. Nucl. Mater. (PSI 1998).
[4] D. Reiter, EIRENE Code Manual, www.eirene.de (1992).
[5] P.C. Stangeby, Physics of plasma wall interactions in controlled fusion, in: D. Post, R. Behrisch (Eds.), NATO ASI Series, Plenum, New York, 1986, and R.Chodura, ditto.
[6] R. Chodura, Physics of plasma wall interactions in controlled fusion, in: D. Post, R. Behrisch (Eds.), NATO ASI Series, Plenum, New York, 1986.
[7] P.C. Stangeby, Nucl. Fus. 32 (12) (1992).
[8] D.S. Gray, M. Baelmans, J.A. Boedo et al., Phys. Plasmas 6 (7) (1999) 2816–2825.
[9] J.H. Ferziger, P. Milovan, Computational Methods for Fluid Dynamics, Springer, Berlin, 1997.